KSCE Journal of Civil Engineering (2018) 22(5):1872-1881

DOI 10.1007/s12205-017-1763-7

Structural Engineering

pISSN 1226-7988, eISSN 1976-3808
www.springer.com/12205

Calculation of RC Flat Slabs and Flat Foundations Punching Using Mini-Max Principle

I. Iskhakov* and Y. Ribakov**

Received October 28, 2016/Revised April 12, 2017/Accepted May 25, 2017/Published Online August 31, 2017

Abstract

The punching problem of reinforced concrete flat slabs and flat foundations has two main aspects, related to load carrying capacity of these structures under shear forces. The first is obtaining the shear force value, and the second – finding the control area (failure zone dimensions). Generally, the punching shear force is taken, based on experimental data, and the control perimeter is assigned according to existing design codes. At the same time, the assigned control perimeter is different for flat slabs and flat foundations. The available experimental and finite element analysis data, used for assigning this area, has a wide scatter and differs by 40-50% from the values, given in modern design provisions. The present study is focused on the above-mentioned second aspect and deals with exact evaluation of the control perimeter under shear punching in flat slabs and flat foundations. This study emphasizes the difference between punching shear due to concentrated load and support reaction force to distributed one. These both cases are investigated using mini-max principle: the internal shear forces are maximized and the control perimeter dimension leads to minimal external load. Efficiency of the proposed method is demonstrated by numerical examples and comparison with available data, based on results of experiments and finite element analyzes. The obtained results can be used as a basis for refinement of existing punching shear models and further development of modern design provisions in this field.

Keywords: *punching shear, flat slab, flat foundation, mini-max principle, reinforced concrete*

1. Introduction

Punching problem of two - way Reinforced Concrete (RC) flat slabs and foundations is widely investigated since the middle of previous century (Kinnunen and Nylander, 1960; Yitzhaki, 1966). Punching acts along some perimeter in flat slabs and flat foundations around columns, which apply concentrated actions or reactions. It yields failure due to localized shear forces along the above - mentioned perimeter.

A well known model for design of flat slab – column and flat foundation – column joints to punching under symmetric loading was proposed by Kinnunen and Nylander (1960). This model was developed later, considering correlation between punching resistance and flexural strength (Yitzhaki, 1966). The size effect in punching shear strength was described by an approximate formula, using a corresponding law for brittle failure (Bazant and Zao, 1987).

It was reported later that punching shear models are based either on empirical and simplified analytical techniques or on theory of plasticity (Yankelevsky and Leibowitz, 1999). A model, based on rigid post-fractured behavior, utilizing the post fracture properties of concrete at the rough crack interfaces, was developed. It was reported that the model predicts the force - displacement resistance during punching. It was shown that the model prediction is in good correspondence with experimental results. However, the kinematic ultimate equilibrium method that was used, is not suitable for brittle behavior of concrete structure under shear forces, because for such behavior the shear force value will not be constant under any finite displacement.

A method for punching shear design of slab - column connections, subjected to seismic loading, was proposed (Brown S. and Dilger, 2004). Following this method, the punching shear design is based on the connection moment capacity, yielding a flexural failure mode that corresponds to a ductile failure mechanism of the connection. A modified yield line approach was presented. The predictions of this moment capacity were compared with available results from the literature.

For analyzing punching shear behavior of RC structures, a two dimensional equivalent continuum model was extended to three dimensional finite element formulation (Ahmad and Tanabe, 2013). It was concluded that a crack angle Θ value of 45° is a good approximation for the average of all crack surface roughness. As concrete stress-strain curves shift from a uniaxial pattern, the concrete peak stresses in three directions were selected correspondingly. It was reported that the numerical results are in good agreement with available experimental data

*Professor, Dept. of Civil Engineering, Ariel University, Ariel University, Ariel 40700, Israel (E-mail: yizhak@ariel.ac.il)
**Professor, Dept. of Civil Engineering, Ariel University, Ariel University, Ariel 40700, Israel (Corresponding Author, E-mail: ribakov@ariel.ac.il)

on load – deflection behavior of RC slabs (Hegger and Beutel, 1998). In this test a hexagonal specimen, supported by 12 rods, was loaded at the center by a hydraulic jack. No shear reinforcement was provided in the slab.

A theoretical background to punching shear provisions of the *fib* Model Code for Concrete Structures (Federation Internationale du Beton, 2012) and an example of their application was presented by Muttoni *et al.* (2013). The mechanical model that forms the basis for the punching design equations was explained. The relevance of the provisions was justified and their suitability for structural design was demonstrated.

To develop the design guidelines and accurate prediction of Steel Fibred Reinforced Concrete (SFRC) flat slabs punching resistance, a database from 154 punching tests was used (Moraes Neto *et al*., 2013). The proposed method is based on the critical shear crack theory that is suitable to investigate the strength of slabs with shear reinforcement (Fernandez Ruiz and Muttoni, 2009). The method is capable to predict the slab load - rotation behavior, considering recommendations of CEB-FIP Model Code for modelling post-cracking behavior of SFRC (CEB: CEB-FIP Model Code, 1991).

Research was performed to study shear mechanisms that govern the behavior of RC structures subjected to localized impact loads (Micallef *et al*., 2014). Such phenomenon is due to combination of inertial and material strain-rate effects, leading to a stiffer slab behavior under higher loading rates. It can also lead to pure punching shear failure, instead of flexural one. The approach that was proposed considers the dynamic punching shear capacity, inertial and material strain-rate effects and demonstrated good correlation with experimental data.

Although there is a lot of experimental and numerical data on flat slab – column joints, similar investigations of flat foundation – column joints is rather limited. Behavior of RC column footing, laid on deformable subgrade and loaded by concentrated load until failure, was recently modeled and analyzed by Vacev *et al.* (2015). Field test data were used for model calibration. Comparison of the experimental and numerical results showed good agreement, but also revealed some questions regarding finite elements analysis.

As known, there are three types of internal forces in the punching failure zone (between the control perimeter and the column): shear forces, radial and tangential bending moments (Kinnunen and Nylander, 1960). The influence of these forces on stress-strain state of the plate within the control perimeter was investigated by Reiss (1994). It was assumed that the control perimeter passes through a section with zero radial moments. In this case, the shear forces contribution (weight coefficient) is about 85% of the total external load and the remained 15% is the weight coefficient of tangential moments. The control perimeter crack inclination angle relative to horizontal plane is assumed to be from 35 to 45°. However, the critical control perimeter value was suggested to be half of the slab thickness. It should be mentioned that those assumptions are based on engineering experience and are not proved.

In the last years the influence of compressive membrane forces action or catenary action effects and moment redistribution is also investigated. It was shown that the behavior of flat slabs depends on the contributions of moment redistributions and compressive membrane actions (Cantone *et al*., 2016). Punching shear tests on slabs with and without shear reinforcement, different reinforcement ratios and loading conditions were carried out. The numerical results were post – processed to adopt the critical shear crack theory failure criterion. Differences between standard specimens and actual members, showing how the current codes of practice underestimate the punching capacity, were reported.

Belletti *et al*. (2016) have studied the behavior of RC slab strips subjected to transverse loads and axial tensile forces. The aim was to investigate the capability of the adopted models and their main influencing parameters. For this reason, validation of suitable numerical tools is useful for a reliable structural robustness assessment. Importance of benchmark development, especially for specimens, in which both mechanical and geometrical nonlinearities play an important role, was underlined.

Compressive membrane action increases the bending and punching capacities of reinforced concrete structures (Belletti *et al*., 2015). A non-linear finite element approach was carried out using ABAQUS Code. Post-processing exploited the critical shear crack theory to evaluate the punching shear resistance of shell elements. The capability of the proposed numerical procedure was checked by comparing numerical predictions with experimental punching shear capacities for tested circular slabs. The same procedure was adopted to punching shear resistance under concentrated loads.

2. Analysis of Modern Codes Provisions on Punching

The punching problem includes various cases from the viewpoint of possible static schemes of flat slabs and foundations, resisting to punching (Fig. 1), and available approaches, related to this problem (Table 1). Part of research results, related to this issue, were discussed in the previous chapter. This chapter analyzes the punching problem from the viewpoint of modern design codes.

The current codes (BR 52-101-2003, 2004; Eurocode , 2004; IS 466, 2003, etc.) are mainly focused on obtaining the value of punching shear force and control perimeter dimensions, as shown in Fig. 2. According to modern design provisions, the punching zone control perimeter is symmetric in case of symmetric external forces. Shear forces and radial moments act along this perimeter. In these codes shear forces are calculated using empirical coefficients, which are different. It is because concrete shear strength in each code is determined, based on different experimental investigations and assumptions. For example, in building rules (BR 52-101-2003, 2004), concrete shear strength is assumed equal to its tensile one. In our opinion, it is because exact data on concrete shear strength is not available. The static scheme for punching calculation according

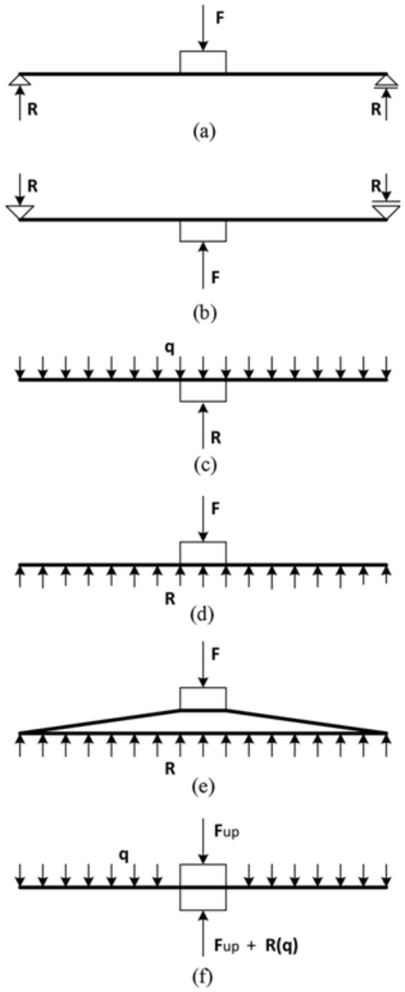

Fig. 1. Static Schemes for Calculation of Problems Related to Punching (a), (b), (c) and (f) - External Load Acts on a Slab with Concentrated Reactions, (d) Same, with Uniformly Distributed Ones

to this code corresponds to Fig. 1(a).

Another problem is selecting the control perimeter location, which following different codes has a wide spread of values (Table 1). Following the table, this spread is between 0.5 *d* and 2.0 *d*, where *d* is the effective flat slab section height. The control perimeter radial crack inclination angle relative to horizontal plane, θ, varies from 19º to 45º. The BR 52-101-2003, 2004 and the *fib* Model Code 2010 recommend to use the value of 0.5 *d* (corresponding to θ = 25.56º).

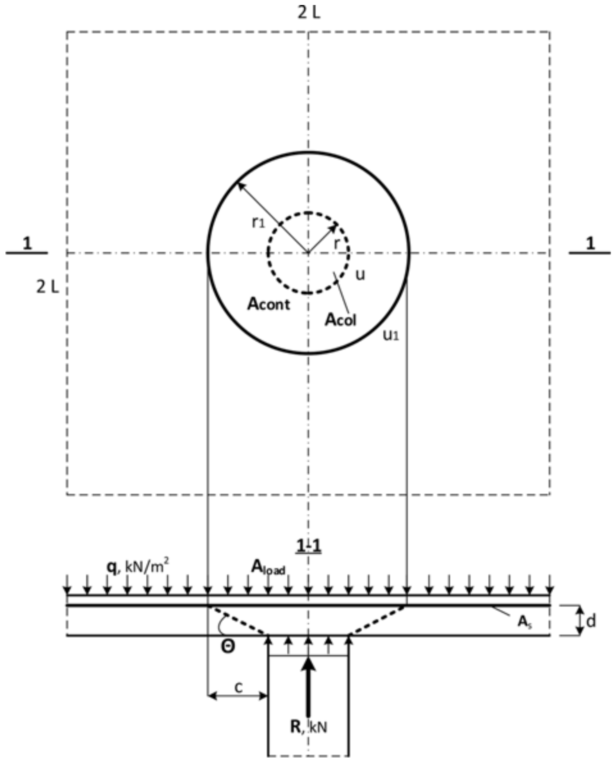

Fig. 2. A General Scheme for Calculations, Related to Punching Problem

Following EC 2 (2004), the control perimeter is 2.0 *d*. The code assumes static schemes, corresponding to Fig. 1(c) and (e) for slabs and foundations, respectively. For slabs and foundations with variable thickness (row 4 in Table 1) θ ≥ arctan 0.5 (θ ≥ 25.56º). For concentrated external force, V_d, the reduced load, applied to the foundation plate, $V_{d.red}$, is decreased by the force, ΔV_d, caused by soil contact pressure

Table 1. Available Data on Crack Inclination Angle and Control Perimeter

No.	Code or reference	Static scheme (following Figure 1)	Application suitability	Limits of angle θ, º	Distance between control perimeter, *u*, and column	Notes
1	BR	1a	Slabs and foundations	26.6	0.5 *d*	-
2	EC 2, CEB, IS 466 – 1	1c	Slabs	25 … 45	2.0 *d*	-
3	IS 466 – 1	1d	Foundations	-	1.0 *d*	*h* = const
4	EC 2	1e	Foundations	≥ arctan 0.5	-	*h* = various
5	Model Code 2010, Muttoni *et al*. (2013)	1b	Slabs	-	0.5 *d*	-
6	Ahmad *et al*. (2013)	1a	Slabs	45*	1.0 *d**	FE mesh
7	Yankelevsky *et al*. (1999)	1a	Slabs	25 … 32	slightly less than 2.0 *d*	-
8	Reiss (1994)	1c	Slabs	35 … 45	0.5 *d*	-

Notations: *u* – control perimeter; *d* – effective flat slab section height; *h* – foundation plate thickness; θ – control perimeter crack inclination angle relative to horizontal plane.
* the values were calculated by the authors.

within the control perimeter, i.e.

$$V_{d.red} = V_d - \Delta V_d \quad (1)$$

The code assumes that the distance 2.0 *d* that characterizes the control perimeter determines the minimal resistance of the plate to the external force.

Following the above - mentioned codes, it can be concluded that the punching control perimeter is not calculated, but assumed within (0.5 … 2.0) *d*. The expressions for concrete shear bearing capacity and the links along the control perimeter are empirical and include many coefficients, based on available experimental data. The existing codes do not define any difference between flat slab – column and column – flat foundation problems, as shown in Fig. 1: in the first case there is a concentrated load, and in the second one – a uniformly distributed reaction.

3. Aims, Scope and Novelty

According to available publications and normative documents, dealing with punching problem, there are no strong analytical dependences for calculating the control perimeter location. It causes uncertainties regarding the shear links' location. Usually shear links are placed according to engineering experience and the available experimental data (Iskhakov *et al*., 2009).

The present study is focused at finding an accurate solution of the punching shear problem, related to the control perimeter value. Strong analytical dependencies are proposed with this aim. Numerical examples demonstrate efficiency of the proposed approach and the analytical results are compared with available experimental and finite element analysis data.

In this study, two main calculation schemes, related to punching shear problem, are considered:

– external load that acts on a slab with concentrated reactions (see Fig. 1(a), (b), (c) and (f));
– external load that acts on a slab with uniformly distributed reaction (see Fig. 1(d) and (e));

The paper deals with analysis of the above - mentioned calculation schemes. It enables to solve the punching problem separately for the cases of flat slab and flat foundations. For solving this problem, mini-max principle was applied (Iskhakov, 2001; Iskhakov and Ribakov, 2014a) considering ultimate limit state analysis (Iskhakov and Ribakov, 2015).

At the same time, taking into account that punching failure is brittle, it is proposed to use steel fibers within the punching control perimeter (see Fig. 6). Efficiency of using steel fibers in preventing brittle failure of concrete was demonstrated previously (Iskhakov and Ribakov, 2013, 2014b).

4. Punching Shear Analysis Using Mini-max Principle

4.1 Main Concepts of Mini-max Principle

The mini-max principle was developed for solving problems, related to finding the load bearing capacity of RC structures, using kinematic or static method of ultimate equilibrium. A mathematical apparatus of this principle is based on the games theory (Karlin, 1959), especially a zero sum game. As static parameter can be selected, for example, the section compressed zone depth and the maximum load bearing capacity of the structure is realized by minimizing the external load, determined by the failure zone dimension (kinematic parameter).

The essence of the mini-max principle is that real load bearing capacity of the structure is calculated (without under- and over-estimation). With this aim, both extreme features of failure load are used simultaneously. At the same time, just one method is used (static or kinematic). Thus, the mini-max principle became a way for realizing the unity theorem of the limit equilibrium method, which joints the static and kinematic approaches.

As it was shown previously, the mini-max principle enables to solve some problems in structural load bearing capacity that had no solutions or were solved approximately (Iskhakov I. and Ribakov, 2014a). The principle is used in the frame of the present study for solving a new problem, related to accurate analysis of RC flat slab and flat foundation punching shear capacity.

As concrete punching shear leads to brittle failure, this special case in mini-max principle requires additional discussion. The kinematic ultimate equilibrium method is not applicable, as concrete, resisting shear forces, has no yield plateau. Therefore, there is no unit displacement, for which the internal and external forces' works are constant. A similar case, when the kinematic method is not applicable, is calculating the load bearing capacity of concrete structures under shear forces.

In such a case, it is possible to use just the static ultimate equilibrium method, when the internal force reaches its ultimate value corresponding to strength of the material, and this value is used in static equilibrium equation. Thus, a two-parametric model becomes a single-parametric one and the problem reduces to finding the maximum internal force value. There is no need in minimization of structural bearing capacity by kinematic ultimate equilibrium method, when static calculation is used, as selection of the most critical section, for which the equilibrium equation is considered, corresponds to minimization of structural bearing capacity by external load.

4.2 Main Assumptions

To allow proper analysis of available data for punching shear calculations, the following main assumptions are used in the present study:

– The vertical concentrated load that yields punching, acts on the slab without eccentricity, i.e. the control perimeter is symmetric relative to the column;
– There is no shear reinforcement, i.e. concrete takes the whole shear force;
– The influence of tangential bending moments is neglected;
– The slab failure due to radial bending moments is excluded;
– as the value of V_{Rdc} is related to the main tensile stresses, it is suggested that the concrete shear resistance is equal to its

tensile strength (this approach is used, for example, in BR 52-101-2003 (2004)).

4.3 Calculation of Punching Shear Due to Concentrated Load

When a slab is subjected to concentrated load, following Figs. 1(a) (and 1(b)), it is assumed that the shear force is taken by concrete, which equals in this case to the shear strength, f_{Vd}. A corresponding shear force is equal to V_{Rdc} (Figs. 3(a) and 4(a)). The shear force is assumed to be uniformly distributed over the entire calculated punching section, $u_1 d$ (Fig. 4(b)).

A corresponding equilibrium equation governs vertical components of these forces, V_{Rdc} sin Θ, and the entire internal force that resists the concentrated external loading is equal V_{Rdc} sin Θ × $u_1 d$ (see Fig. 4(b)). Therefore, the forces equilibrium equation in vertical direction takes the following form:

$$F_{Rd} = \Sigma V_{Rdc} \sin \Theta \quad (2)$$

and ΣV_{Rdc} acts along a circular control perimeter, u_1, with radius r_1:

$$\Sigma V_{Rdc} = f_{Vd}\, d\, u_1;\; u_1 = 2\pi\, r_1 = 2\pi\, (d \cot \Theta + r) \quad (3)$$

where r is the column section radius.

Then

$$\Sigma V_{Rdc} = 2\pi\, d f_{Vd}\, (d \cot \Theta + r) \quad (4)$$

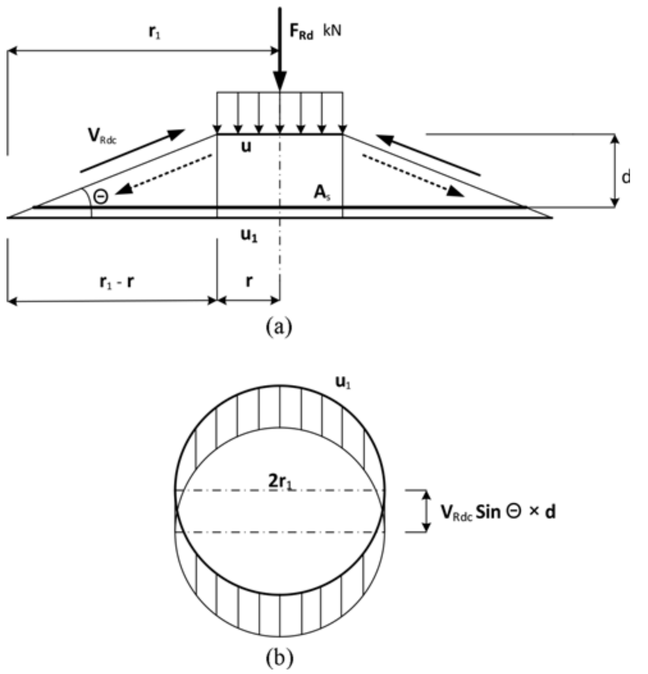

Fig. 4. Calculation Scheme of Punching Shear, Corresponding to Fig. 1(a) (and 1(b)).

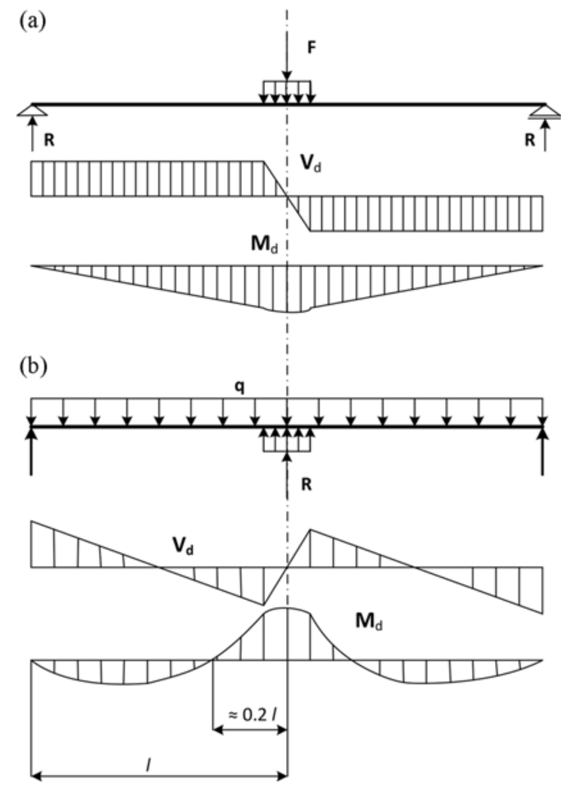

Fig. 3. Diagrams of Shear Forces and Bending Moments: (a) Corresponding to Schemes "a" and "b" in Fig. 1; (b) - to Schemes "c" … "f".

This force is equivalent to the external load F_{Rd}. Hence, from Eq. (2) follows that

$$F_{Rd} = 2\pi\, d f_{Vd}\, (d \operatorname{co} \Theta + r) \sin \Theta \quad (5)$$

It is convenient to use this expression in the following form:

$$F_{Rd} = 2\pi f_{Vd}\, d^2\, [\cos \Theta + (r/d) \sin \Theta] \quad (6)$$

Theoretically the value of angle Θ (see Fig. 4) is within the following limits: $0 \le \Theta \le 90^o$.

Defining

$$F_{Rd}^{*} = (r/d) \sin \Theta + \cos \Theta \quad (7)$$

yields

$$F_{Rd} = 2\pi\, d^2 f_{Vd}\, F_{Rd}^{*} \quad (8)$$

For example, for $r = d = 15$ cm (when the effective slab depth is equal to the column section radius), Θ = 45º and f_{Vd} = 1 MPa, $F_{Rd}^{*} = \sqrt{2}$ and F_{Rd} = 199929.7 N = 199.93 kN. The radius of the control perimeter $r_1 = d \cot \Theta + r$ = 30 cm, i.e. the control perimeter diameter is 60 cm. If $F_{Rd} < F_d$, it is necessary to provide shear reinforcement along the control perimeter. Here F_d is an external design force (shown as F in the figures).

Mini-max analysis of Eq. (8) yields to maximization of the function, as the shear forces are constant, according to the diagram shown in Fig. 3(a):

$$\frac{dF_{Rd}^{*}}{d\vartheta} = -d \sin \Theta + r \cos \Theta = 0 \quad (9)$$

Hence

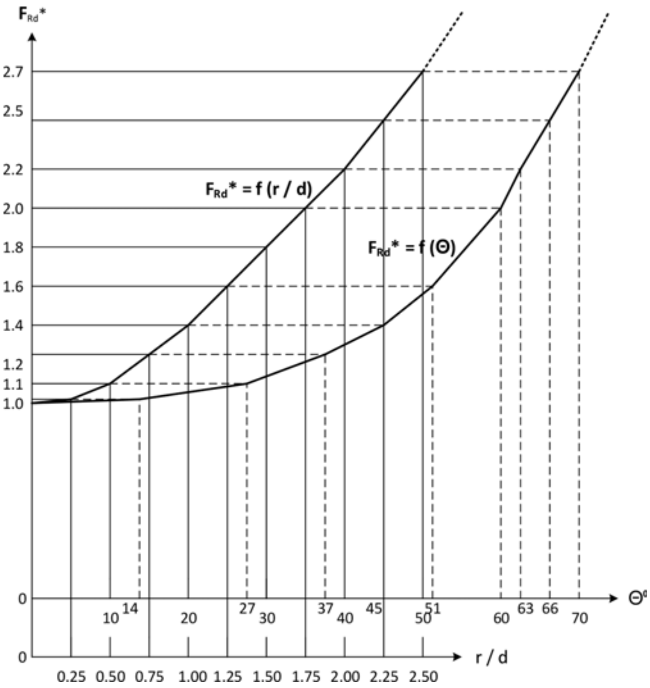

Fig. 5. Graphs of F_{Rd}^* vs. *r*/*d* and F_{Rd}^* vs. Θ°

$$\tan \Theta_{extr} = r/d;\ \Theta_{extr} = \arc\tan (r/d) \quad (10)$$

The second derivative of Eq. (9) is:

$$\frac{d^2 F_{Rd}^*}{d\vartheta^2} = -d \cos \Theta - r \sin \Theta \quad (11)$$

Taking into account that theoretically $0^0 \le \Theta \le 90^0$, the second derivative is negative, therefore the function has a maximum. Practically, maximum values of F_{Rd}^*, corresponding to physical limits of Θ, should be taken, according to the graphs, shown in Fig. 5 (or in Table 2).

Analysis of F_{Rd}^* vs. *r*/*d* is presented in Table 2. The values of *r*/*d* varied within its limits (mathematically from 0 to ∞ and physically from 0.25 to 2.5). As it follows from the table, as the ratio *r*/*d* increases, the values of angle Θ and F_{Rd}^* become higher

Table 2. Analysis of F_{Rd}^* = cos (arc tan *r*/*d*) + (*r*/*d*) sin (arc tan *r*/*d*)

r / d	Θ° = arc tan r/d	$r_1 - r = d \cot \Theta$	F_{Rd}^*
0.00	0.0	∞	1.000
0.25	14.0	4.04 *d*	1.030
0.50	26.6	2.0 *d*	1.119
0.75	36.9	1.33 *d*	1.125
1.00	45.0	1.00 *d*	1.417
1.25	51.3	0.80 *d*	1.600
1.50	56.3	0.67 *d*	1.800
1.75	60.3	0.57 *d*	2.019
2.00	63.4	0.50 *d*	2.228
2.25	66.1	0.45 *d*	2.463
2.50	68.2	0.40 *d*	2.696
∞	90.0	0.00	∞

and correspondingly, according to Eq. (8), the flat slab load bearing capacity, F_{Rd}, also grows. Fig. 5 presents functions F_{Rd}^* vs. *r*/*d* and F_{Rd}^* vs. Θ. Theoretically, the maximum values of both functions correspond to $r/d = \infty$, but practically they are limited by physical values of *r* and *d*.

To verify the efficiency of the proposed method, available data for a flat slab, presented by Ahmad and Tanabe (2013), was analyzed. Twelve tie rods were used to provide vertical supports of the hexagonal specimen, loaded on the center column with a hydraulic jack (bottom-up testing). The slab width was 275 cm. The slab thickness $h = 23$ cm and its effective depth $d = 19.5$ cm. No shear reinforcement was provided in the slab. It is also given that the column section dimensions are 40 × 40 cm, i.e. the inscribed circle radius $r = 20$ cm. Taking into account that the concrete shear strength $f_{Vd} \approx f_{ct} = 1.73$ MPa [16] and considering that according to Table 2, for $r/d \approx 1$, yields $\Theta = 45°$, $r_1 = 2\,r$, $F_{Rd}^* = \sqrt{2}$. Then, according to Eq. (8), $F_{Rd} = 2\sqrt{2}\,\pi\ 195^2\ 1.73 = 582498$ N = 582.5 kN. According to the experimental result (Ahmad and Tanabe, 2013), the limit load of the slab in punching is 600 kN, which is in perfect agreement with the theoretical result, obtained using the proposed methodology.

Thus, a practical method for accurate calculation of a flat slab punching shear capacity due to concentrated load is proposed for a case when no shear reinforcement is required. At the same time, the control perimeter of the punching failure zone is obtained (it corresponds to $r_1 = r + d \cos \Theta$). In case, when the flat slab punching shear capacity is not sufficient, shear reinforcement should be added along the control perimeter. This reinforcement should be calculated, according to the concentrated load

$$\Delta F_d = F_d - F_{Rd} \quad (12)$$

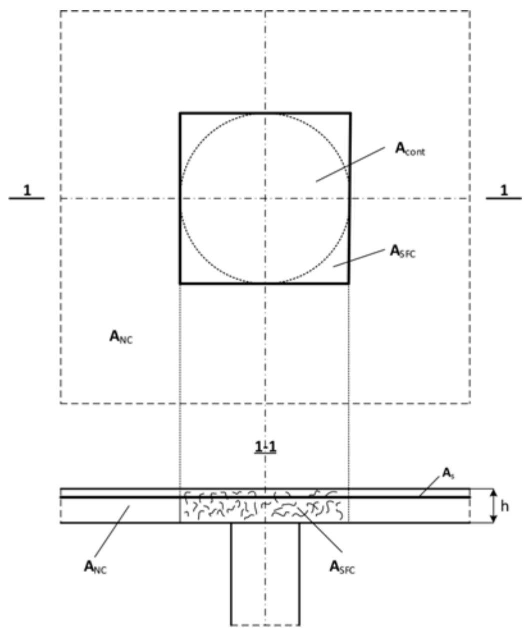

Fig. 6. Using Steel Fibred Concrete Within the Punching Control Perimeter

To prevent brittle failure due to punching shear, steel fibers can be used within the control perimeter (Fig. 6). Calculation of optimal steel fibre content can be performed according to the concept that was previously developed by Iskhakov and Ribakov (2013).

4.4 Calculation of Punching Shear Due to Distributed Load and Support Reaction

When a slab is subjected to uniformly distributed load and reaction, following Figs. 1(c), (d) and (f), it is also assumed that the shear force is taken by concrete, which equals to the shear strength, f_{Vd}. A corresponding shear force is equal to V_{Rdc} (Fig. 3(b) and 7(a)). The shear force is assumed to be uniformly distributed over the entire calculated punching section, $u_1 d$ (Fig. 7(b)). In this case, the forces equilibrium equation has the following form:

$$q_{Rd} + \Sigma V_{Rdc} \sin \Theta = R_d \quad (13)$$

where R_d is the support reaction.

Performing similar perturbations, like in case of punching shear due to concentrated load, this equation can be re-written as follows:

$$[(r/d) + \cot \Theta]^2 q_{Rd} + 2 f_{Vd} [(r/d) \sin \Theta + \cos \Theta] = R_d/(\pi d^2) \quad (14)$$

Here

$$R_d = V_d = k\, l_x\, l_y\, q_{Rd} \quad (15)$$

where k is a coefficient, representing the relation between the support reaction and the external load (depending on the flat slab static scheme with spans l_x and l_y). For example, for a symmetric slab that has two spans in x and y directions, for inner column, k = 1.25.

Substitution of Eq. (15) into (14) yields:

$$q_{Rd} = \frac{2 f_{Vd}\left(\frac{r}{d}\sin\theta + \cos\theta\right)}{\frac{k l_x l_y}{\pi d^2} - \left(\frac{r}{d} + \cot\theta\right)^2} \quad (16)$$

For real values of r/d and Θ (see Table 2) the second term in the denominator is significantly less than the first one, therefore, the second term is neglected and Eq. (16) takes the following form:

$$q_{Rd} = \frac{2\pi d^2 f_{Vd}\left(\frac{r}{d}\sin\theta + \cos\theta\right)}{k l_x l_y} \quad (17)$$

Defining

$$q_{Rd}^* = \frac{r}{d}\sin\theta + \cos\theta \quad (18)$$

yields

$$q_{Rd} = \frac{2\pi d^2 f_{Vd}}{k l_x l_y}\, q_{Rd}^* \quad (19)$$

The first derivative of this expression enables to find the value of

$$\Theta_{extr} = \arctan (r/d) \quad (20)$$

Then

$$q_{Rd}^* = \frac{r}{d}\sin\left(\arctan\frac{r}{d}\right) + \cos\left(\arctan\frac{r}{d}\right) \quad (21)$$

The second derivative of Eq. (19) is negative for all practical values of Θ, therefore the function has a maximum.

To verify the efficiency of the proposed method, available data for a flat slab, presented by Muttoni (2013), was analyzed. The slab has two bays in each direction. The contributing area of the inner column is $l_x \times l_y$ = 6.0 × 5.6 m. The slab thickness h = 25 cm and its effective depth d = 20.0 cm. It is also given that the column section dimensions are 26 × 26 cm, i.e. r = 13 cm. Taking into account that for concrete strength class C30/37, f_{ck} = 30 MPa. The uniformly distributed load, acting on the slab, $q_d = V_d/(l_x \times l_y)$ = 19.8 kN/m², the reaction in the inner column R_d = 664 kN. The control perimeter was suggested to be 1668 mm, which corresponds to a distance of $r_1 - r = d/2$ = 10 cm from the supported area (Muttoni *et al.*, 2013) that corresponds to Θ = 26.6°.

Following BR 52-101-2003(2004) and Eurocode (2004), the concrete shear strength $f_{Vd} = f_{ct} \approx f_{ck}/10$ = 3.0 MPa. According to Table 2, for r/d = 13/20 = 0.65 yields Θ = 33°, q_{Rd}^* = 1.122. Then, following Eq. (19),

$$q_{Rd} = [\, 2\pi\, 200^2\, 3.0/(1.25\ 6000\ 5600)]\ 1.122 = 21.4 \text{ kN/m}^2$$

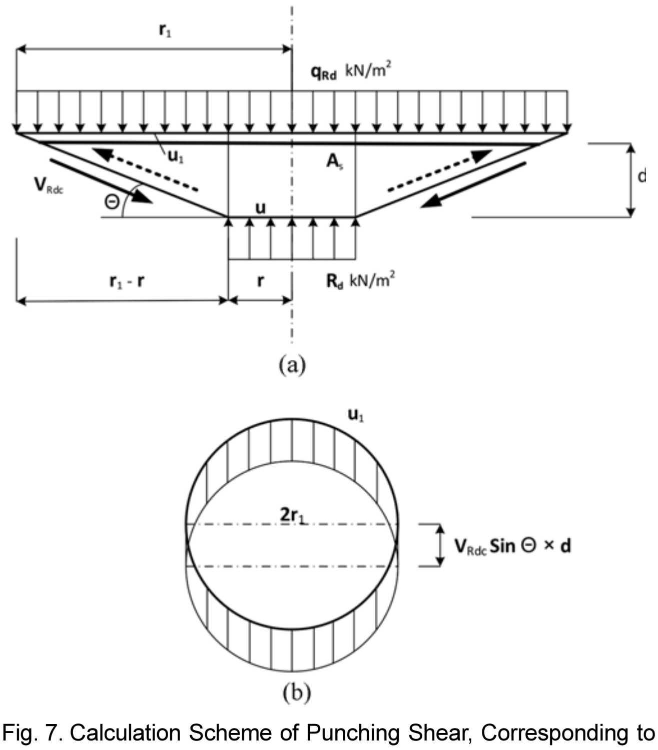

Fig. 7. Calculation Scheme of Punching Shear, Corresponding to Fig. 1(c) (and 1(d), (f)).

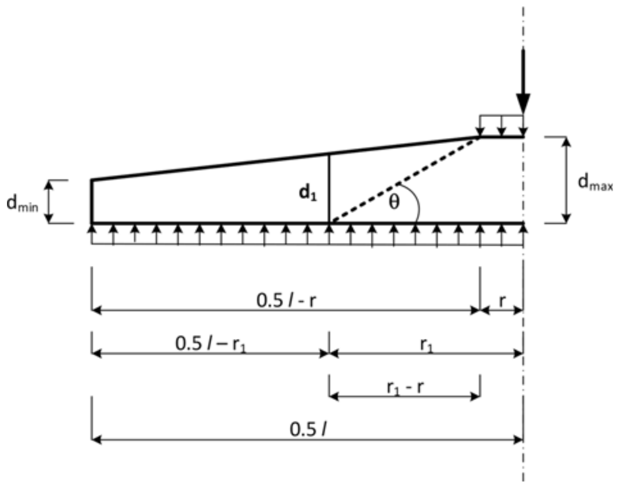

Fig. 8. Calculation Scheme of Punching Shear, Corresponding to Fig. 1(e)

This result is close to that, obtained by finite element analysis (Muttoni *et al*., 2013) (q_d = 19.8 kN/m^2).

$r_1 - r = d \cot \Theta = 15.4 \text{ cm} = 0.77\, d$

In case if the flat slab punching shear capacity is not sufficient, shear reinforcement should be added along the control perimeter, which should be accurately determined as 0.77 *d*.

4.5 Calculation of Punching Shear Due to Distributed Load and Support Reaction in Flat Foundation with Variable Thickness

In case of a flat foundation with variable thickness the scheme corresponds to that, shown in Fig. 1(e). Calculation of this structure is similar to that, described in section 4.4, i.e. the basic expression is Eq. (13) and the final one is Eq. (17). However, the effective section depth is variable, i.e. $d_1 = f(\Theta)$, as shown in Fig. 8.

The additional variable d_1 is obtained according to the following dependence:

$$\frac{d_1 - d_{\min}}{d_{\max} - d_{\min}} = \frac{0.5\, l - r_1}{0.5\, l - r} \quad (22)$$

Taking into account that in this case

$$r_1 = r + d_{\max} \cot \Theta \quad (23)$$

after simple mathematical perturbations, Eq. (22) takes the following form:

$$d_1 = d_{\min} + \left(1 - \frac{d_{\max} \cot\theta}{0.5\, l - r}\right)(d_{\max} - d_{\min}) \quad (24)$$

5. Particular Cases in Design to Punching Using Mini-max Principle

Following Eq. (6), characterizing the flat slab load bearing capacity to punching, F_{Rd}, depends on three variable values: *d*, *r* and Θ. Taking into account that Θ is a function of *d* and *r*, some private cases, related to the ratio *r*/*d*, can be solved using mini-max principle. If the ratio *r*/*d* is known, then a minimum of the function Θ(*r*/*d*) is known. In this case the mini-max problem turns to finding a maximum of this function. Let consider the following private cases.

Case 1: given *r* and *d*. Then defining the expression in the brackets from Eq. (6) by F_{Rd}^* then

$$F_{Rd} = 2\pi f_{Vd}\, d^2\, F_{Rd}^*;\ F_{Rd}^* = \cos \Theta + (r/d) \sin \Theta \quad (25)$$

If, for example, *r/d* = 1 then

$$F_{Rd}^* = \cos \Theta + \sin \Theta \quad (26)$$

and the maximum of this function is at

$$d\, F_{Rd}^*/d\, \Theta = -\sin \Theta + \cos \Theta = 0 \quad (27)$$

or

$$\sin \Theta = \cos \Theta;\ \Theta = 45^0 \quad (28)$$

Then going back to Eq. (25),

$$F_{Rd} = 2\pi f_{Vd}\, d^2\, F_{Rd}^* = 2\sqrt{2}\, \pi f_{Vd}\, d^2 \quad (29)$$

In a common case, when *r* = *k d*, where according to available experimental data and modern codes (see Table 1) *k* varies from 0.5 to 2,

$$F_{Rd}^* = \cos \Theta + k \sin \Theta \quad (30)$$

$$d\, F_{Rd}^*/d\, \Theta = -\sin \Theta + k \cos \Theta = 0 \quad (31)$$

and

$$\text{tg}\, \Theta = k \quad (32)$$

Case 2: given *d* and the values of *r* and Θ are unknown. In this case, a mini-max problem is solved again based on Eq. (30). As there are two unknowns and it is known that the structure indeed reaches the ultimate limit state, it can be assumed that

$$F_{Rd} = F_d \quad (33)$$

where F_d is a known external concentrated load. Then according to Eq. (25)

$$F_d = 2\pi f_{Vd}\, d^2\, F_{Rd}^* \quad (34)$$

i.e.

$$F_{Rd}^* = F_d/(2\pi f_{Vd}\, d^2) \quad (35)$$

Thus, F_{Rd}^* is a known value and from Eq. (30) follows

$$F_{Rd}^* - \cos \Theta = (r/d) \sin \Theta \quad (36)$$

In this case, the maximum condition in the mini-max principle is satisfied according to Eq. (33) and therefore minimization problem is solved for the function *r* (Θ), i.e. d *r*/d Θ = 0.

$$r = d\,(F_{Rd}^*/\sin \Theta - \cot \Theta) \quad (37)$$

$$dr/d\, \Theta = -\frac{F_{Rd}^* \cos\theta}{\sin^2\theta} - \left(-\frac{1}{\sin^2\theta}\right) = 0 \quad (38)$$

Therefore

$$\cos \Theta = 1/F_{Rd}^{*} \quad (39)$$

and from Eq. (37) follows that

$$r_{opt} = (d/\sin \Theta)\,(F_{Rd}^{*} - \cos \Theta) \quad (40)$$

Case 3: given r whereas d and Θ are unknown. The problem is solved like in case 2.

6. Conclusions

Punching of reinforced concrete flat slabs and flat foundations has two main aspects: obtaining the shear force value, and finding the control perimeter that defines the failure zone dimension. According to most available methods, the control perimeter is assigned and not calculated, but the problem is that this perimeter is different for flat slabs and flat foundations. Moreover, available data, used in modern design codes for assigning this perimeter, has a wide scatter (up to 40-50%).

In the frame of the present study, an accurate and rather simple method for evaluation of the control perimeter under shear punching in flat slabs and flat foundations is proposed. The difference between punching shear due to concentrated load and support reaction force due to distributed one is shown. Both cases are investigated using mini-max principle, the concept of which is described in the paper. For analyzing the punching shear capacity, the static method of structural ultimate equilibrium is used. The kinematic parameter is taken, based on the most critical section from the punching shear viewpoint.

The proposed method allows calculation of the control perimeter dimension and avoids the need for assuming it, like in existing design codes. As punching failure is brittle, it is proposed to add steel fibre within the control perimeter. It is also shown that the proposed methodology can be applied for calculating flat foundations with variable thickness.

Efficiency of the proposed method is demonstrated in numerical examples. The obtained results are compared with available experimental and numerical data. It is shown that the proposed method enables to predict the control perimeter dimension and the ultimate load on the flat slab and flat foundation with high accuracy. It allows finding a more exact location of shear links in flat slabs, if it is necessary according to calculation.

As examples of the proposed method application, private cases of punching shear design are solved, using mini-max principle. The differences between the experimental data and theoretical predictions, based on mini-max principle, are 2.9% for punching shear due to concentrated load and 7.5% for distributed load. In a general case, taking into account the experimental data scatter for RC structures, this accuracy is suitable.

The proposed method can be used as a basis for improving the existing punching shear models and further development of modern design provisions for punching.

References

Ahmad, S. I. and Tanabe, T. (2013). "Three-dimensional FE analysis of reinforced concrete structures using the lattice equivalent continuum method." *Structural Concrete Journal of the fib*, Vol. 1, No. 14, pp. 51-59.

Bazant, Z. P. and Zao, O. (1987). "Size effect in punching shear failure of slabs." *ACI Structural Journal*, Vol. 84, No. 1, pp. 44-53.

Belletti, B., Damoni, C., Cervenka, V., and Hendriks, M. A. N. (2016). "Catenary action effects on the structural robustness assessment of RC slab strips subjected to shear and tensile forces." *Structural Concrete*, Vol. 17, No. 6, pp. 1003-1016.

Belletti, B., Walraven, J. C., and Trapani, F. (2015). "Evaluation of compressive membrane action effects on punching shear resistance of reinforced concrete slabs." *Engineering Structures*, Vol. 95, No. 7, pp. 25-39.

BR 52-101-2003 (2004). *Non-pre-stressed concrete and reinforced concrete structures*, NIIZhB, Moscow.

Brown, S. and Dilger, W. (2004). "Design of slab - column connections to resist seismic loading, 13th World Conference on Earthquake Engineering." Vancouver, Canada, August 1-6, Paper No. 2832.

Cantone, R., Belletti, B., Manelli, L., and Muttoni, A. (2016). "Compressive membrane action effects on punching strength of flat RC slabs." *Key Engineering Materials*, Vol. 711, pp. 698-705, *8th International Conference on Concrete under Severe Conditions - Environment and Loading*, Lecco, Italy, 12-14 September.

CEB (1990). *CEB-FIP Model Code 1990 – Final draft,* Bulletin Nos. 203-205. Comite Euro-international du Beton, Lausanne.

Eurocode 2 (2004). *Design of Concrete Structures – Part 1-1: General Rules and Rules for Buildings*.

Federation Internationale du Beton (2012). *Model Code 2010, final draft,* Bulletin 65, Lausanne, Switzerland.

Fernandez, Ruiz M. and Muttoni, A. (2009). "Applications of critical shear crack theory to punching of reinforced concrete slabs with transverse reinforcement." ACI *Structural Journal*, Vol. 106, No. 4, pp. 485-494.

Hegger, J. and Beutel, R. (1998). *Durchstanzen schubbewehrter Flachdecken im Bereich von Innenstutzen*, Final report, AiF research project 10644N, Chair and Institute of Concrete Structures, RWTH Aachen University (in German).

IS 466 Concrete Code (2003). *General Principles, Part 1*, The Standards Institution of Israel.

Iskhakov, I. (2001). "Quasi-isotropic ideally elastic-plastic model for calculation of RC elements without empirical coefficients." *Structural Engineering, Mechanics and Computation,* Vol. I, Elsevier, pp. 367-374.

Iskhakov, I., Ribakov, Y., and Shah, A. (2009). "Experimental and theoretical investigation of column – flat slab joint ductility." *Materials and Design*, Vol. 30, No. 8, pp. 3158-3164.

Iskhakov, I. and Ribakov, Y. (2013). "A new concept for design of fibered high strength RC elements using ULS method." *Materials and Design*, Vol. 51, pp. 612-619.

Iskhakov, I. and Ribakov, Y. (2014a). *Ultimate equilibrium of RC structures using mini-max principle*, Nova Publishers.

Iskhakov, I. and Ribakov, Y. (2014b). "Exact solution of shear problem for inclined cracked bending reinforced concrete elements." *Materials and Design*, Vol. 57, pp. 472-478.

Iskhakov, I. and Ribakov, Y. (2015). "Ultimate limit state of pre-stressed reinforced concrete elements." *Materials and Design*, Vol. 75, pp. 9-16.

Karlin, S. (1959). *Mathematical Methods and Theory in Games, Programming and Economics,* Pergamon Press, London/Paris.

Kinnunen, S. and Nylander, H. (1960). *Punching of concrete slabs without shear reinforcement*, Transaction, Nr. 158, KTH, Stockholm.

Micallef, K., Sagaseta, J., Fernández, Ruiz M., and Muttoni, A. (2014). "Assessing punching shear failure in reinforced concrete flat slabs subjected to localized impact loading." *International Journal of Impact Engineering*, Vol. 71, pp. 17-33.

Moraes, Neto B., Barros, J., and Melo, G. (2013). "A model for the prediction of the punching resistance of steel fibre reinforced concrete slabs centrically loaded." *Construction and Building Materials*, Vol. 46, pp. 211-223.

Muttoni, A., Fernandez, Ruiz M., Bentz, E., Foster, S., and Sigrist, V. (2013). "Background to *fib* Model Code 2010 shear provisions – part II: Punching shear." *Structural Concrete Journal of the fib*, Vol. 3, No. 14, pp. 204-214.

Reiss, M. (1994). *Reinforced Concrete Slabs*, Michlol (in Hebrew).

Vacev, T., Bonić, Z., Prolović, V., Davidović, N., and Lukić, D. (2015). "Testing and finite element analysis of reinforced concrete column footings failing by punching shear." *Engineering Structures*, Vol. 92, No. 1, pp. 1-14.

Yankelevsky, D. Z. and Leibowitz, O. (1999). "Punching shear in concrete slabs." *International Journal of Mechanical Sciences*, Vol. 41, No. 1, pp. 1-15.

Yitzhaki, D. (1966). "Punching strength of reinforced concrete slabs." *ACI Journal*, Vol. 63, No. 5, pp. 527-542.